Proteophosphoglycans of *Leishmania mexicana*

Identification, purification, structural and ultrastructural characterization of the secreted promastigote proteophosphoglycan pPPG2, a stage-specific glycoisoform of amastigote aPPG

Christian KLEIN, Ulrich GÖPFERT, Nathan GOEHRING, York-Dieter STIERHOF and Thomas ILG[1]

Max-Planck-Institut für Biologie, Abteilung Membranbiochemie Corrensstrasse 38, D-72076 Tübingen, Germany

Protozoan parasites of the genus *Leishmania* secrete a range of proteophosphoglycans that appear to be important for successful colonization of the sandfly and for virulence in the mammalian host. A hallmark of these molecules is extensive phosphoglycosylation by phosphoglycan chains via the unusual linkage $Man\alpha 1$-PO_4-Ser. In this study we have identified and purified to apparent homogeneity a novel proteophosphoglycan (pPPG2) which is secreted by *Leishmania mexicana* promastigotes (sandfly stage). Amino acid analysis and immunoblots using polypeptide-specific antisera suggest that pPPG2 shares a common protein backbone with a proteophosphoglycan (aPPG) secreted by *Leishmania mexicana* amastigotes (mammalian stage). Both pPPG2 and aPPG show a similar degree of Ser phosphoglycosylation (50.5 mol % vs. 44.6 mol %), but the structure of their phosphoglycan chains is developmentally regulated: in contrast to aPPG which displays unique, complex and highly branched glycan chains [Ilg, Craik, Currie, Multhaup, and Bacic (1998) J. Biol. Chem. **273**, 13509–13523], pPPG2 contains short unbranched structures consisting of > 60 mol % neutral glycans, most likely $(Man\alpha 1$-$2)_{0-5}Man$ and $Gal\beta 1$-$4Man$, as well as about 40 mol % monophosphorylated glycans of the proposed structures PO_4-$6Gal\beta 1$-$4Man$ and PO_4-$6(Glc\beta 1$-$3)Gal\beta 1$-$4Man$. The major differences between pPPG2 and aPPG with respect to their apparent molecular mass, their ultrastructure and their proteinase sensitivity are most likely a consequence of this stage-specific glycosylation of their common protein backbone.

Key words: electron microscopy, O-glycosylation, phosphoserine.

INTRODUCTION

Protozoan parasites of the genus *Leishmania* infect two groups of host organisms, the vector sandflies and mammals. In sandflies the parasites colonize the lumen of the digestive system, whereas in the mammalian host they reside in the phagolysosomal compartment of macrophages. Different *Leishmania* species cause several diseases in humans ranging from relatively benign cutaneous ulcers to fatal visceral spread of the parasites [1].

The search for *Leishmania* molecules important for successful colonization of the sandfly gut by the insect stage parasites, the promastigotes, and of macrophages by the mammalian stage parasites, the amastigotes, has indicated that complex glycoconjugates may play a major role in the infection process. Parasite glycans identified to date include the dominant glycosylphosphatidylinositol (GPI) anchored cell surface glycoproteins leishmanolysin (gp63) [2] and gp46/psa2 [3,4], the highly abundant glycoinositolphospholipids (GIPLs) [5–9] and a range of parasite compounds containing unique phosphorylated oligosaccharides. This family of phosphoglycan-modified molecules [10] consists of the unconjugated phosphoglycan (PG [11,12]), the lipid-linked lipophosphoglycan (LPG, reviewed in [13,14]) and several protein-linked phosphoglycans collectively termed proteophosphoglycans (PPGs, reviewed in [15,16]).

The complex promastigote cell surface glycolipid LPG was the first phosphoglycan discovered [11,17,18] and its detailed structure has been elucidated for several *Leishmania* species [19–23].

Its conserved backbone is formed by a 1-*O*-alkyl-2-*lyso*-phosphatidyl *myo*-inositol lipid anchor, a diphosphoheptasaccharide core, phosphodiester-linked [PO_4-6-$Gal\beta 1$-$4Man\alpha 1$-] repeating units and a neutral oligosaccharide cap. Species- and life-stage variability exists in the Gal-3-OH and Man-2-OH substitutions of the repeats and in the details of the cap structure. LPG is the dominant cell surface molecule of *Leishmania* promastigotes and its presence may be crucial for the survival of the parasites in the sandfly and in the mammalian host. Potential functions of LPG include its action as a ligand for insect midgut and macrophage receptors, the formation of a protective surface glycocalyx against the action of insect digestive enzymes and macrophage phagolysosomal hydrolases, inhibition of complement lysis and phagosome–lysosome fusion, and impairment of macrophage activation by inhibition of protein kinase C and other signalling pathways. Structure–function analyses have indicated that all LPG structure elements, in particular the phosphosaccharide repeats and the neutral cap oligosaccharides, confer biological activity (reviewed in [10,13–16,24]).

In the case of PPGs, phosphosaccharide repeats and cap glycans are linked to a protein backbone via phosphodiester linkages to serine, an unusual form of protein glycosylation termed phosphoglycosylation [25–28]. The group of PPGs consists primarily of secreted parasite products such as acid phosphatase (SAP [25,29–32]), filamentous proteophosphoglycan from promastigotes (fPPG [26,33]) and a non-filamentous proteophosphoglycan from amastigotes (aPPG [27,34]). Recently,

however, a cell surface membrane-bound PPG with a putative GPI anchor has been identified on *L. major* promastigotes [35] and ultrastructural studies suggest that PG-modified molecules may also be abundant in the extended lysosomes of *L. mexicana* amastigotes [36,37]. The precise functions of most of these PPGs for the parasites remain elusive; however, recent studies have provided some clues. fPPG appears to be important for efficient transmission of *Leishmania* promastigotes from the sandfly to the mammalian host ([38], and references therein), while aPPG has been shown to be an extremely potent activator of complement via the mannose-binding lectin pathway [39] and to induce vacuole formation in the host cells of *Leishmania*, the macrophages [40a].

In this study, we describe the identification, purification and structural characterization of a previously unknown PPG from *L. mexicana* promastigotes which we call pPPG2. We provide biochemical evidence that the pPPG2 protein backbone is identical to that of aPPG from amastigotes of the same *Leishmania* species. This result is corroborated by molecular cloning and targeted deletion of the *L. mexicana* aPPG gene [40b]. Our analyses suggest that while the degree of Ser phosphoglycosylation is similar in pPPG2 and aPPG, stage-specific modifications of the glycan chains lead to major differences of their molecular masses, ultrastructures and protease sensitivities.

MATERIALS AND METHODS

Parasites

Promastigotes of *L. mexicana* MNYC/BZ/62/M379 (wild type, WT) were grown *in vitro* in semi-defined medium 79 supplemented with 5 % heat-inactivated fetal bovine serum (iFCS) as previously described [41]. For some experiments a *L. mexicana* mutant in which both genes encoding secreted acid phosphatase have been deleted (*L. mexicana* Δlmsap1/2, [42]) were used. Cells were harvested at densities of 5×10^7–10^8/ml. Culture supernatant was stored at 4 °C after the addition of 0.1 % (w/w) of NaN_3 to prevent bacterial and fungal growth. To preserve the virulence of *L. mexicana* WT, the parasites were isolated at 3-month intervals from dorsal lesions CBA/J or C57/Bl6 mice infected 3–6 months previously in the rump at the base of the tail with 10^7 stationary phase promastigotes.

Antisera

Eight C57/Bl6 mice were immunized with native aPPG (50 μg) and with aPPG that had been deglycosylated by mild acid hydrolysis (200 μg) [27]. For primary immunizations and booster immunizations, the compounds were resuspended in 0.5 ml 50 % complete or 0.5 ml 50 % incomplete Freund's adjuvant in phosphate-buffered saline, pH 7.3 (PBS), respectively. The mice were bled 10–14 days after each booster immunization. The immune sera of one mouse (M1.1) showed a strong reactivity against aPPG previously deglycosylated by 40 % HF treatment [27] and was used for immunoblot experiments (this study) and antibody screening of λ-phage expression libraries of *L. mexicana* cDNA [40b].

Analytical procedures

Discontinuous SDS/polyacrylamide electrophoresis (SDS/PAGE [43]) was performed on 4 % stacking gels over 7.5–20 % separating gels. After electrophoresis gels were stained either with Coomassie Blue to detect proteins or with Stains-all to detect PG-containing compounds as well as proteins [25,44]. For electrotransfer of proteins from SDS/polyacrylamide gels

[44] polyvinylidene difluoride (PVDF) membranes (Millipore, Eschborn/Germany) were used. For immunodetection of antigens on PVDF membranes, nonspecific binding sites were blocked for 1 h at 25 °C in 50 mM Tris/HCl pH 7.5, 150 mM NaCl, 5 % skim milk powder, 0.1 % Tween-20 (TBS/MT). The monoclonal mouse antibody (mAb) LT6 (IgG1, hybridoma supernatant), which recognizes the PO_4-6-Galβ1–4Manα1-PG repeats, mAbs L7.25 and AP3 (IgM, ascites fluids), which recognize the PG cap structures $(Man\alpha1–2)_{0–2}Man\alpha1-PO_4$- [44], the mAb L3.13 (IgG1, ascites fluid) which recognizes a PG epitope present on *Leishmania* proteophosphoglycans, but not LPG [33,44], mAb LT8.2, which is directed against a peptide epitope of SAP phosphatase (IgG2a, hybridoma supernatant) and rabbit antisera against the C-terminal non-repetitive aPPG domain expressed as hexa-His-tagged protein in *E. coli* (see [40b]) were used as primary antibodies at dilutions of 1:20, 1:1000, 1:2 and 1:200, respectively, in TBS/MT. After 3 washes with 50 mM Tris/HCl pH 7.5, 150 mM NaCl, 0.1 % Tween-20 (TBS/T), goat anti-mouse IgG or goat anti-rabbit IgG antibodies coupled to alkaline phosphatase or horseradish peroxidase (Dianova) were used at a 1:10000 dilutions in TBS/MT. After 5 washes with TBS/T, the bound enzyme conjugates were detected either by colour development using 0.5 mM 5-bromo-4-chloro-3-indolylphosphate and 0.5 mM nitrobluetetrazolium dissolved in 50 mM $NaHCO_3$/NaOH, 2 mM $MgCl_2$, pH 9.6, or by chemiluminescence using either CDP-Star (Perkin–Elmer) or the ECL detection system (Amersham–Pharmacia). Proteinase K digests prior to SDS/PAGE were performed in sample buffer. Dephosphorylation of PPGs for SDS/PAGE immunoblot analysis or glycan analysis was performed by incubating salt-free samples with 50 μl 40 % HF at 0 °C for 48–60 h [27]. Total phosphate content was determined as described previously [23] and the protein concentration was estimated by the bicinchoninic acid assay according to the manufacturer's instructions (Pierce).

Purification of aPPG and pPPG2

L. mexicana aPPG was purified from mouse lesion tissue as described earlier [34,39]. For the purification of pPPG2, *L. mexicana* promastigote (WT or Δlmsap 1/2) culture supernatant (1–2 l) was loaded onto a DE52 cellulose column (25 × 1.5 cm) at a flow rate of approx. 2 ml/min. After washing the column with 200 ml 100 mM NaCl, 20 mM Tris/HCl pH 7.5, elution was performed by a linear gradient of 100 ml 100–500 mM NaCl in 20 mM Tris/HCl pH 7.5. PPGs in the eluate were detected by phosphate determination and by two-site ELISA using purified mAb L7.25 as capture antibody and LT6, LT8.2 or biotinylated L7.25 as detecting antibodies. The bound detection antibodies were vizualized by goat anti-mouse IgG (γ-chain-specific)-alkaline phosphatase or Extravidin-alkaline phosphatase and pNPP as a chromogenic substrate as outlined earlier [25]. In the case of *L. mexicana* WT, fractions were also analysed for SAP activity [31]. Fractions positive in the SAP assay and/or in ELISA were pooled, adjusted to 1 M $(NH_4)_2SO_4$ and loaded onto an octyl-Sepharose column (15 × 1.5 cm) equilibrated with 1 M $(NH_4)_2SO_4$, 20 mM Tris/HCl, pH 7.5 at a flow rate of 1 ml/min. After washing with 60 ml 1 M $(NH_4)_2SO_4$, 20 mM Tris/HCl pH 7.5, the column was further eluted with 40 ml 20 mM Tris/HCl, pH 7.5. Fractions were analysed as described above. The octyl-Sepharose unbound material was subjected to ultracentrifugation (40000 rev./min, 3 h, Beckman Ti60 rotor, 4 °C). The ultracentrifugation supernatant was carefully separated from the pellet and concentrated about 100-fold by ultrafiltration using Centriprep 10 and Centricon 10 devices according to the manufacturer's instructions (Amicon, Witten,
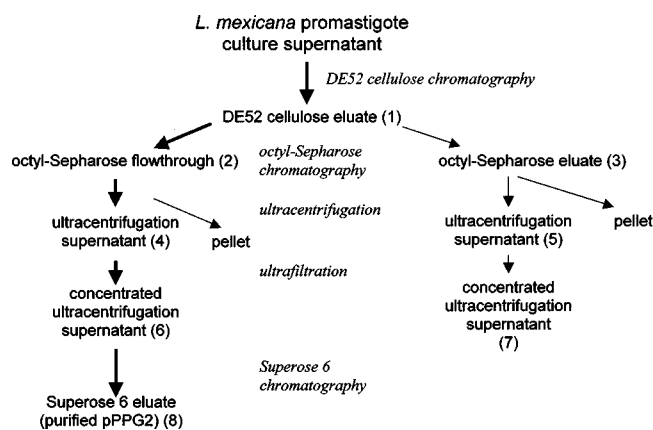
Scheme 1 Flow diagram of pPPG2 purification from *L. mexicana* promastigote culture supernatant

The numbers in parentheses indicate the fractions analysed by SDS/PAGE and SDS/PAGE/immunoblot in Figure 4. The strong arrow indices the direction leading to purified pPPG2.
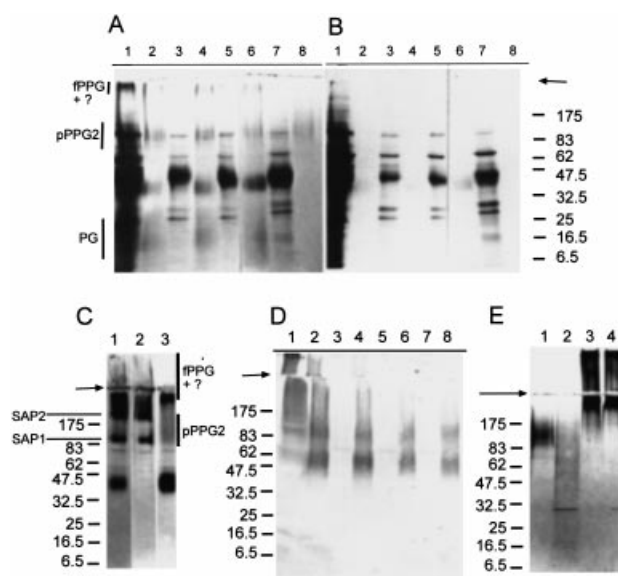

Figure 1 Analysis of pPPG2 purification and protease sensitivity by SDS/PAGE and SDS/PAGE/immunoblot

(**A**, **B**) SDS/PAGE/Stains-all staining (**A**) and SDS/PAGE/Coomassie Blue staining (**B**) of 0.25% (v/v) (lanes 1–5) or 0.5% (v/v) (lanes 6–8) samples of the different pPPG2 purification steps. Lane 1, DE52 cellulose eluate; 2, octyl-Sepharose flowthrough; 3, octyl-Sepharose eluate; 4, ultracentrifugation supernatant of the octyl-Sepharose flowthrough; 5, ultracentrifugation supernatant of the octyl-Sepharose eluate; 6, as lane 4 but concentrated by ultrafiltration; 7, as lane 5 but concentrated by ultrafiltration; 8, purified pPPG2 after Superose 6 chromatography. (**C**) SDS/PAGE/Stains-all staining of ultracentrifugation fractions from the octyl-Sepharose flowthrough of *L. mexicana* WT; 0.25% (v/v) samples of the fractions were loaded. Lane 1, octyl-Sepharose flowthrough; 2, ultracentrifugation pellet of lane 1; 3, ultracentrifugation supernatant of lane 1. (**D**) SDS/PAGE/immunoblot of the different pPPG2 purification steps with mouse antiserum 1.1; loading of the gel as in (**A**) and (**B**). (**E**) SDS/PAGE/Stains-all staining of proteinase K-treated pPPG2 and aPPG. Lane 1, pPPG2 — proteinase K; 2, pPPG2 + proteinase K; 3, aPPG — proteinase K; 4, aPPG + proteinase K.

Germany). The concentrated samples were loaded onto a Superose 6 gel filtration column equilibrated with 250 mM ammonium acetate, eluted at a flow rate of 0.5 ml/min. The fractions were analysed for SAP activity and by two-site ELISA

as described above and were also inspected by electron microscopy (see below). Fractions containing pPPG2 were pooled and concentrated by Centricon 10 ultrafiltration.

Amino acid and phosphoamino acid analysis

Amino acid analysis was performed after hydrolysis of PPG samples (1–10 μg protein) with 100 μl 6 N HCl (Pierce) containing 0.1% phenol *in vacuo* at 110 °C for 20 h. After evaporation of the acid, the dried hydrolysates were converted to phenyl-thiocarbamyl derivatives and analysed by reversed phase HPLC (RP-HPLC) on a Pico-Tag column (Waters, Eschborn, Germany) using the conditions described earlier [45]. Amino acid standard solutions (Sigma) were treated in the same way to correct for losses during hydrolysis. To detect Ser(P), PPG samples (5–20 μg protein) were subjected to partial acid hydrolysis (100 μl 6 N HCl containing 0.1% phenol, 110 °C, 60–90 min *in vacuo*). Following the conversion to phenylthiocarbamyl derivatives, RP-HPLC was performed using the above conditions except for changing the pH of the 300 mM NaAc buffer from 6.5 to 5.5 and raising the temperature to 50 °C. Phosvitin, Ser(P) and Thr(P) (Sigma) were used as standard compounds [26]. Under these conditions Ser(P) eluted just before Asp, Thr(P) just after Glu. To quantitate Ser(P) in PPGs, the phosphoamino acid was converted to S-ethylcysteine (SEC) by alkaline β-elimination in the presence of ethanethiol [46]: dried salt-free PPG samples were incubated with 30 μl of 13.2% (v/v) ethanol, 9.9% (v/v) ethanethiol, 10.7% (v/v) 5 M NaOH (v/v), 66.2% H_2O (v/v) for 1 h at 50 °C. The samples were cooled on ice, neutralized by the addition of 7.5 μl acetic acid and dried under a stream of N_2 and in a Speed Vac evaporator (Savant). After acid hydrolysis (100 μl 6 N HCl containing 0.1% phenol, 110 °C, 20 h *in vacuo*), S-ethylcysteine was determined as a phenylthiocarbamyl derivative as described above. Amino acid standard solutions (Sigma) complemented with SEC (Sigma) were treated in the same way to correct for losses during hydrolysis. In some experiments the PPG samples were treated with alkaline phosphatase or were deglycosylated by mild acid hydrolysis followed by incubation with alkaline phosphatase [26] prior to β-elimination and hydrolysis.

Analysis of glycans

Phosphorylated and neutral glycans were released from pPPG2, aPPG, SAP or LPG by mild acid hydrolysis or by incubation in 40% HF [27] and separated using a high pH anion exchange HPLC (HPAE-HPLC) system (GP40, ED40, Dionex, Idstein, Germany) on a Carbo-Pac PA10 column (4 × 250 mm, Dionex) by linear sodium acetate gradients formed in 100 mM NaOH solutions. Program 1 (0 mM for 6 min, to 50 mM over 18 min, to 125 mM over 7 min, held at 125 mM for 4 min) was used for neutral glycans; program 2 (program 1 followed by: to 175 mM over 3 min, held at 175 mM for 3 min, to 250 mM over 20 min and held at 250 mM for 10 min) for neutral and monophosphorylated glycans and program 3 (program 2 followed by: to 1 M over 4 min, held at 1 M for 13 min) for the separation of neutral, mono- and multiphosphorylated glycans. In some experiments glycans were digested with jack bean α-mannosidase or bovine testes β-galactosidase (Roche, Mannheim, Germany) as previously described. Authentic phosphoglycan and neutral glycan standards were isolated from mild acid- and 40% HF-treated *L. mexicana* LPG and SAP [23,25] by HPAE-HPLC. Fractions containing individual glycans were neutralized by the addition of 1/10 vol. 2 M acetic acid, desalted by passage through a 1 ml column of AG50W-X4 (BioRad, München, Germany) and lyophilized.

Electron microscopy

Glycerol spraying, rotary metal shadowing and electron microscopic inspection of purified proteophosphoglycans was performed as described earlier [26,48]. The contour length of fully extended aPPG and pPPG2 filaments were determined by the use of a magnifying lens with measure on 120000-fold photographic enlargements of electron micrographs.

RESULTS

Purification of *L. mexicana* promastigote pPPG2 and identification of its relationship to aPPG from amastigotes

In the course of purification of several already characterized PG-modified molecules (LPG, PG, fPPG, SAP) secreted by *L. mexicana* WT or *L. mexicana* Δlmsap1/2 promastigotes, a previously unknown compound was identified (Scheme 1). Culture supernatant was subjected to anion-exchange chromatography on DE52 cellulose, and PG-containing molecules, as

detected by phosphate determination and two-site ELISA, were eluted from the column by a salt gradient in a broad peak at approx. 200–300 mM NaCl (not shown). The peak contained LPG, PG, fPPG, and SAP (SAP is only present in the case of purifications from *L. mexicana* WT supernatant), as well as various proteins derived from fetal calf serum as judged by SDS/PAGE followed by Stains-all or Coomassie Blue staining (see Figures 1A and 1B, lanes 1). The pooled DE52 cellulose fractions were adjusted to 1 M $(NH_4)_2SO_4$ and loaded onto an octyl-Sepharose column equilibrated in the same buffer. Most contaminating proteins and LPG were retained by the column, whereas PG as well as the bulk of fPPG and SAP (80–90 %) were found in the flowthrough (Figures 1A and 1B, lanes 3, and Figure 1C, lane 1). Some fPPG and acid phosphatase activity (10–20 %) could be eluted from the column by a low salt wash, but they were heavily contaminated with other proteins (Figures 1A and 1B, lanes 3). The flowthrough fractions were subjected to ultracentrifugation. More than 95 % of SAP and a large proportion of the fPPG, Figure 1C, lane 2) was found in the pellet
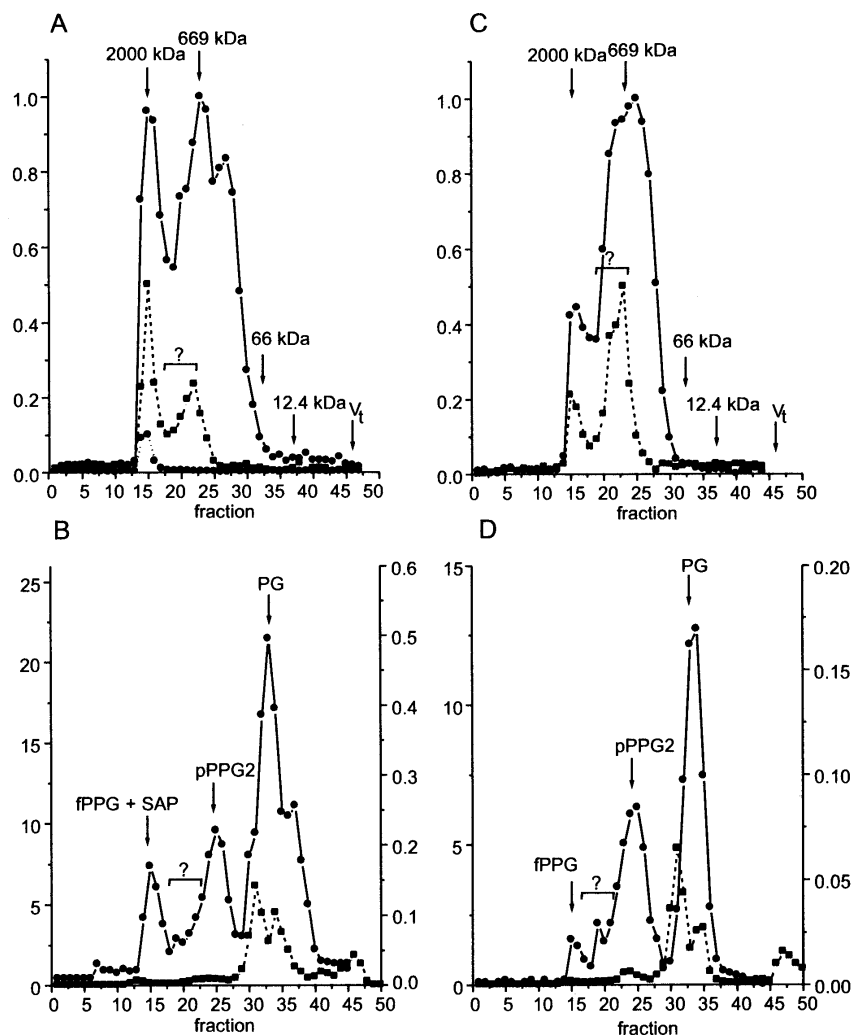
Figure 2   Purification of pPPG2 by Superose 6 chromatography

(**A**, **B**) *L. mexicana* WT; (**C**, **D**) *L. mexicana* Δlmsap1/2. The presence of PG-modified compounds is indicated by the two-site ELISA signal (Figure 2A and 2C, O.D.$_{405}$; L7.25 —●—, LT6 ---■---), the phosphate content (Figure 2B and 2D, O.D.$_{830}$; —●—) and in the case by the acid phosphatase activity (Figure 2A, O.D.$_{405}$; ····●····). The protein content of the fractions was estimated by their O.D.$_{280}$ (Figure 2B and 2D; ---■---). The elution positions of molecular size markers (dextran blue, 2000 kDa; thyroglobulin, 669 kDa; BSA, 66 kDa; cytochrome c, 12.4 kDa and the inclusion volume (sodium azide, V_t) are indicated.

Figure 3   Electron microscopy of glycerol-sprayed and rotary metal shadowed *L. mexicana* PPGS

(**A**) SAP (arrow) and fPPG (arrowhead) from pooled Superose 6 fractions 15/16 of *L. mexicana* WT promastigote culture supernatant (cf. Figure 2A with 2B). (**B**) pPPG2 from pooled Superose 6 fractions 25/26 of *L. mexicana* WT promastigote culture supernatant (cf. Figure 2A with 2B), (**C**) aPPG purified from mouse lesion tissue infected with *L. mexicana* WT amastigotes.

while PG remained soluble (Figure 1A, lane 6, and Figure 1C, lane 3); however considerable amounts of PG-modified molecules with slower elect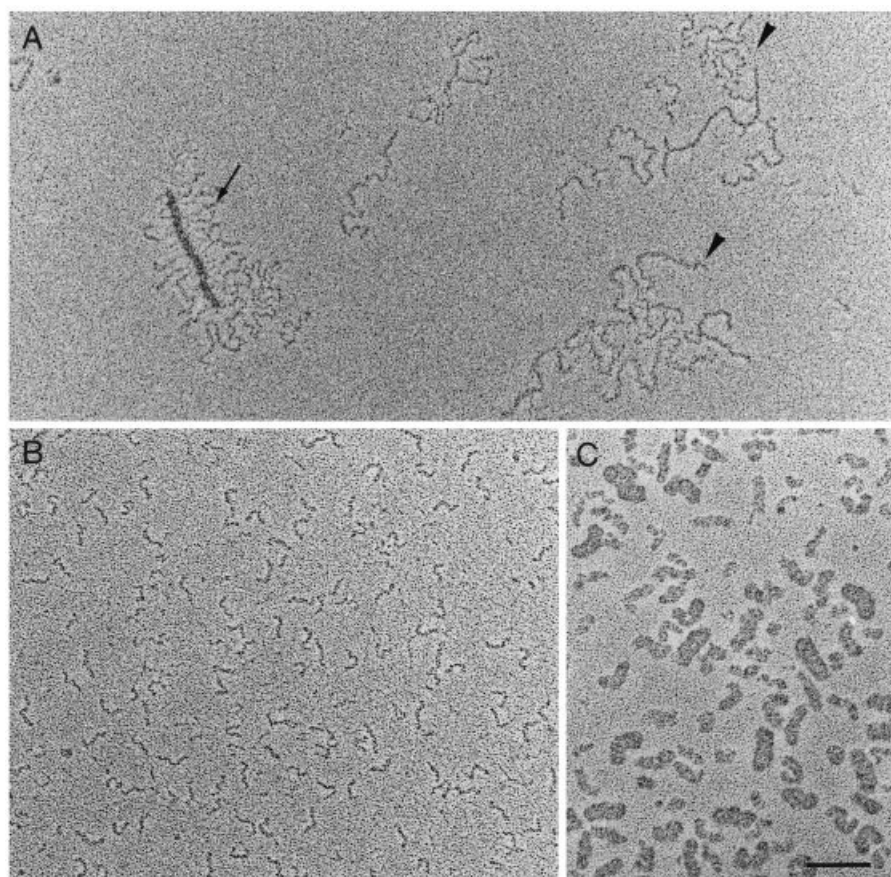rophoretic mobility than PG were also detected in the ultracentrifugation supernatant as indicated by Stains-all staining (Figure 1A, lane 6, Figure 1C, lane 3) and immunoblotting using mAbs L7.25 and AP3 (not shown). To investigate the nature of these molecules, the ultracentrifugation supernatant was concentrated and applied to a Superose 6 gel filtration column. Three PG-containing peaks were identified in purifications from both *L. mexicana* WT and the Δlmsap1/2 mutant by their phosphate content: the peak close to the void volume of the column (Figure 2B and 2D) corresponded to residual fPPG and SAP as judged by two-site ELISA (Figures 2A and 2C), enzyme assay (Figure 2A), electron microscopic inspection (Figure 3A) as well as SDS/PAGE/Stains-all staining (not shown) and SDS/PAGE/immunoblotting (Figure 4A, lanes 14–18). The peak that eluted after the 66 kDa marker (Figures 2B and 2D) was not detected by two-site ELISA or immunoblot (Figure 4A) and consisted of unconjugated PG [11,12]. A third PG-containing peak (Figures 2B and 2D) eluting between SAP/fPPG and PG was observed. The most concentrated fractions of this peak (Figures 2B and 2D, fractions 24–27) exhibited a broad band in between the 175 kDa and the 83 kDa marker in Stains-all stained SDS polyacrylamide gels (not shown) which also reacted strongly with mAbs L7.25 (Figure 4A) and AP3 (not shown).

This compound in Superose fractions 24–27 did not correspond to any known PG-modified *L. mexicana* promastigote product and was named pPPG2. Since immunoblots of native or 40 % HF-treated samples probed with anti-SAP mAb LT8.2 [44] or rabbit antiserum raised against the fPPG protein backbone (anti-HFP serum [26]) did not show any signal, it was considered unlikely that pPPG2 was related to the previously characterized PPGs SAP [44], fPPG [26] or mPPG [35]. Another possibility was a relationship of pPPG2 to a distinct PPG secreted by mammalian stage amastigotes of *L. mexicana* (aPPG [27,34]). To resolve this question antisera were raised in mice by immunization with native and mild acid-deglycosylated aPPG. The presence of specific antibodies was tested by immunoblots of native aPPG and the same molecule that had been deglycosylated by 40 % HF treatment. One mouse serum (M1.1) showed strong reactivity to deglycosylated (Figure 4B, lane 3), but not to native aPPG (Figure 4B, lane 4) whereas the control mAb L7.25 directed against LPG/ PPG mannooligosaccharide caps showed the opposite specificity, as expected (Figure 4B, lanes 1 and 2). This result indicated that the mouse antiserum M1.1 was specific for the aPPG polypeptide backbone and did not recognize the glycan structures found on aPPG, various other PPGs and LPG. pPPG2-containing Superose 6 eluate fractions (Figures 2B and 2D) were treated with 40 % HF, subjected to SDS/PAGE, blotted onto PVDF membranes and probed with mouse antiserum M1.1. A strong reaction was observed with this antiserum and the signal was proportional
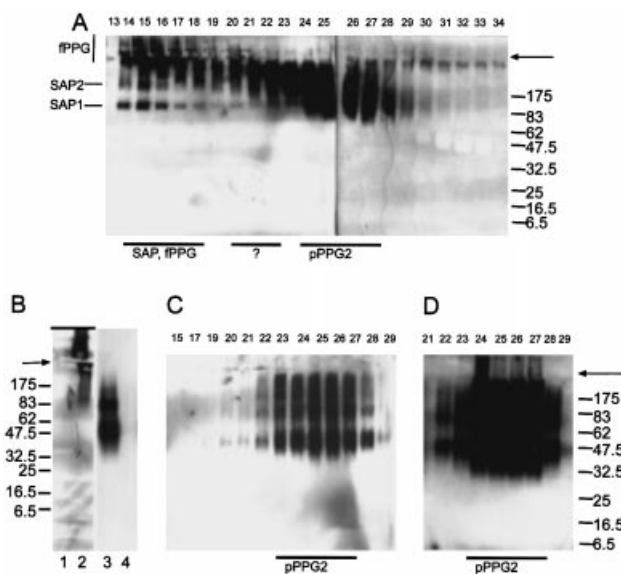
Figure 4   Purification of *L. mexicana* pPPG2 by Superose 6 chromatography: characterization by SDS/PAGE and immunoblotting

(**A**) Ten μl of Superose 6 chromatography fractions (see Figures 2A and 2B) were subjected to SDS/PAGE. After blotting onto a cationized nylon membrane, PG antigens were detected by mAb L7.25. (**B**) Thirty μg of 40% HF-treated (lanes 1, 3) and native (lanes 2, 4) aPPG were subjected to SDS/PAGE, blotted onto a cationized nylon (lanes 1, 2) or a PVDF membrane (lanes 3, 4) and probed with mAb L7.25 (lanes 1, 2) or mouse antiserum M1.1 (lanes 3, 4). (**C**) Twenty μl of 40% HF-treated Superose 6 chromatography fractions were subjected to SDS/PAGE, blotted onto a PVDF membrane and probed with mouse antiserum M1.1. (**D**) as in (**C**), but probed with rabbit anti PPG2 N-terminal/repeat domain antiserum.

Figure 5   Comparison of *L. mexicana* pPPG2 with other *Leishmania* PG antigens by SDS/PAGE and immunoblotting

Native (**A–C**) or 40% HF-treated (**D**) *L. mexicana* pPPG2 (lanes 1), *L. mexicana* aPPG (lanes 2), *L. major* fPPG (lanes 3), *L. mexicana* SAP (lanes 4) and *L. mexicana* LPG (lanes 5) were subjected to SDS/PAGE followed by Stains-all staining (**A**), or immunoblotting using mAb L7.25 (**B**), mAb LT6 (**C**) and mouse antiserum M1.1 (**D**) for detection of antigens.

to the phosphate content of pPPG2-containing fractions (Figure 4C). This indicated that pPPG2 possessed a protein backbone related or identical to that of *L. mexicana* aPPG secreted by lesion amastigotes. This interpretation was confirmed by an immunoblot of the same 40% HF-treated pPPG2-containing fractions (Figures 2B and 2D) with a rabbit antiserum against an *E. coli*-expressed portion of aPPG [40b], which resulted in essentially the same signal pattern (Figure 4D).

Based on the signal intensities on the M1.1-probed immunoblots, fractions 24–27 of the Superose 6 chromatography containing the aPPG-related pPPG2 were pooled and concentrated.

Its purity was assessed on SDS/polyacrylamide gels by staining with Coomassie Blue that binds to contaminating proteins (Figure 1A, lanes 1, 3, 5, 7), but not to pPPG2, by Stains-all staining which preferentially stains phosphoglycosylated products (Figure 1A, lane 8; Figure 5A, lane 1), and by electron microscopy (see below). The relative yields of pPPG2 throughout the purification procedure (Scheme 1) were estimated by scanning of X-ray films exposed to the chemiluminescence signal of mouse antiserum M1.1-probed immunoblots of 40% HF-treated samples of the different purification steps (Figure 1D). A purification factor of more than 23000 based on protein content was achieved with an overall yield of 26% (Table 1). Based on phosphate associated with macromolecules, the purification factor was 235 (Table 1). About 52 μg of pPPG2 were recovered from 2 l of late log phase (6×10^7/ml) *L. mexicana* promastigotes. Since the *L. mexicana* Δlmsap1/2 mutants yielded the identical product in similar yields, the synthesis and secretion of pPPG2 secretion appears to be independent of SAP production.

It should be noted that in the Superose 6 eluate between fPPG/SAP (peak A, Figures 2B and 2D) and pPPG2 (peak C, Figures 2B and 2D) another PPG present in minor amounts was identified (marked by ?, Figures 2 and 4). This compound reacts strongly with mAb L7.25 (Figures 2A and 2C, 4A), but in

Table 1   Purification of pPPG2 from *L. mexicana* promastigote culture supernatant

	pPPG2*	Volume (ml)	Total protein (mg)	pPPG2/ protein	Purification factor pPPG2/protein	Total PO$_4$ μg	pPPG2/ PO$_4$	Purification factor pPPG2/PO$_4$
L. mexicana Δlmsap1/2 culture supernatant	100†	2000	4656	0.021	1	8740	0.0114	1
DE52 eluate	100†	58	32.5	3.077	143	1687	0.0593	5.2
Octyl-Sepharose flowthrough	53.2	79	N.D.	—	—	938	0.0567	5.2
Ultracentrifugation supernatant	42.7	79	N.D.	—	—	837	0.051	4.7
Ultracentrifugation supernatant concentrated by ultrafiltration	29.2	0.065	0.3	97.3	4530	68	0.4294	37.7
Superose 6 fractions 24–27	26.0	2	0.052	500	23 280	9.7	2.6804	235.2

* Arbitrary values determined by densitometry of an immunoblot of 40% HF-treated samples (see Figure 1D).
† The amount of pPPG2 in the DE52 eluate was set as 100, because it could not be quantitated in the culture supernatant.
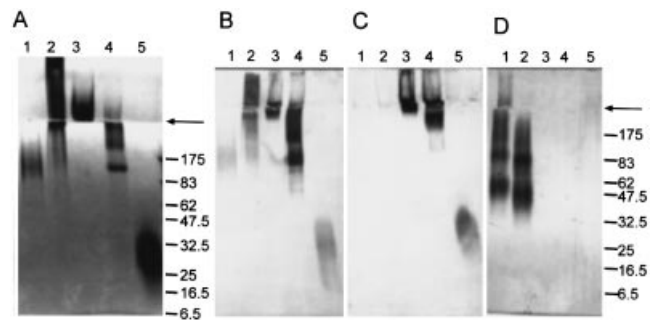N.D., not determined due to the extremely low protein concentration in these samples.

A

B

pPPG2
42.9 nm +/- 3.7 nm (n = 190)
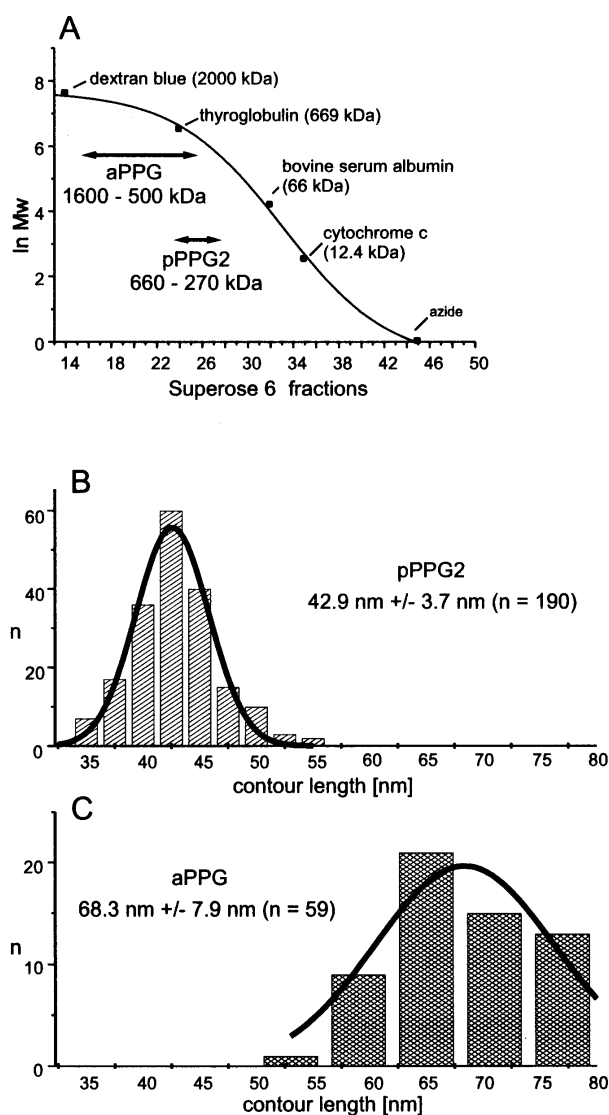
C

aPPG
68.3 nm +/- 7.9 nm (n = 59)

Figure 6   Size comparison of *L. mexicana* pPPG2 and aPPG

The sizes of *L. mexicana* pPPG2 and aPPG were compared by chromatography on a calibrated Superose 6 gel filtration column (**A**) and by direct measurement of the molecules on electron micrographs of glycerol-sprayed and rotary-shadowed samples (**B**, **C**).

Table 2   Amino acid composition of pPPG2 and aPPG

Amino acid	*L. mexicana* pPPG2 [mol %]†	*L. mexicana* aPPG, deduced from the DNA sequence‡	*L. mexicana* aPPG, purified from lesion supernatant§	*L. mexicana* aPPG, purified from isolated amastigotes§
Asp + Asn	3.8 ± 0.2	5.6	5.30	3.50
Glu + Gln	10.5 ± 0.4	9.3	9.70	9.05
Ser	24.4 ± 0.7	23.5	26.95	30.95
Gly	9.9 ± 0.4	11.5	8.15	10.55
His	2.4 ± 0.2	3.2	2.50	2.50
Arg + Thr*	10.3 ± 0.5	11.5	14.15	9.35
Ala	9.8 ± 0.4	10.9	9.45	12.15
Pro	7.9 ± 0.3	3.4	6.60	4.35
Tyr	1.7 ± 0.3	1.4	1.20	1.25
Val	5.4 ± 0.2	5.6	4.30	3.50
Ile	2.0 ± 0.1	1.4	2.45	2.95
Leu	3.7 ± 0.5	4.3	3.65	3.65
Phe	5.4 ± 0.3	5.7	4.45	5.35
Lys	2.7 ± 0.2	2.7	1.05	1.00

* Poorly resolved amino acids.
† Average of 17 determinations, the standard error is indicated.
‡ See ref. [40b].
§ Taken from [34].

lmsap1 and *lmsap2* gene products and a smear extending into the stacking gel corresponding to loosely associated fPPG-like material (Figure 5A, lane 4; [25,32,42]). *L. mexicana* aPPG exhibits the most disperse pattern spanning the entire stacking gel and part of the separating gel to an apparent molecular mass of about 150 kDa (Figure 5A, lane 2). The Stains-all pattern of pPPG2 after SDS/PAGE was distinct from all other PPGs and showed a broad band centred between 83 and 175 kDa apparent molecular mass (Figure 5A, lane 1). On immunoblots pPPG2 showed a reaction with anti-mannooligosaccharide cap mAb L7.25 which reacts with all known PG-modified molecules (Figure 5B). pPPG2, however, did react only very weakly with mAb LT6 directed against the common phosphodisaccharide repeats (Figure 5C) and not at all with mAb LT22 that is directed against glucosylated phosphodisaccharide repeats (not shown). Importantly, after 40 % HF dephosphorylation/deglycosylation both pPPG2 and aPPG were recognized by mouse antiserum M1.1 (Figure 5D, lanes 1 and 2) while fPPG, SAP and LPG were not (Figure 5D, lanes 3–5).

To test their sensitivity against proteolytic cleavage aPPG and pPPG2 were incubated with proteinase K and analysed by SDS PAGE. While aPPG did not show any sign of degradation on Stains-all stained SDS/polyacrylamide gels, pPPG2 was cleaved to a wide range of fragments that appeared as a smear (Figure 1E).

The elution behaviour of aPPG and pPPG2 on Superose 6 gel filtration columns showed some major differences which reflected by their distinct size and ultrastructure, as shown directly by electron microscopy of glycerol-sprayed and rotary-shadowed samples: aPPG eluted early in a broad peak spanning from approx. 1600 to 500 kDa apparent molecular mass, while pPPG2 eluted later in a sharper peak centring between 600 and 270 kDa (Figure 6A). Likewise, in electron microscopy, pPPG2 molecules appeared as a homogeneous population of short thread-like structures with an average length of 42.9 nm ± 3.7 nm and a diameter of about 3–6 nm (Figure 4B). In contrast, aPPG molecules appeared larger and much more heterogeneous in their

contrast to pPPG2 (see below) it also strongly reacts with mAb LT6 (Figures 2A and 2C). Electron microscopic inspection of these Superose 6 fractions indicated the presence of filamentous structures with similar overall morphology as fPPG (see Figure 2A), but with considerably shorter length (200–400 nm). This minor PPG species was not further characterized in this study.

Biochemical and ultrastructural characterization of pPPG2

Purified pPPG2 was compared with other *Leishmania* PPGs and *L. mexicana* LPG by SDS/PAGE/Stains-all staining and by SDS/PAGE/immunoblots using monoclonal and polyclonal antibodies: in Stains-all stained SDS/polyacrylamide gels *L. major* fPPG remains largely in the stacking gel (Figure 5A, lane 3, cf. [26]) while SAP shows two defined bands at approx. 100 and 200 kDa apparent molecular mass corresponding to the
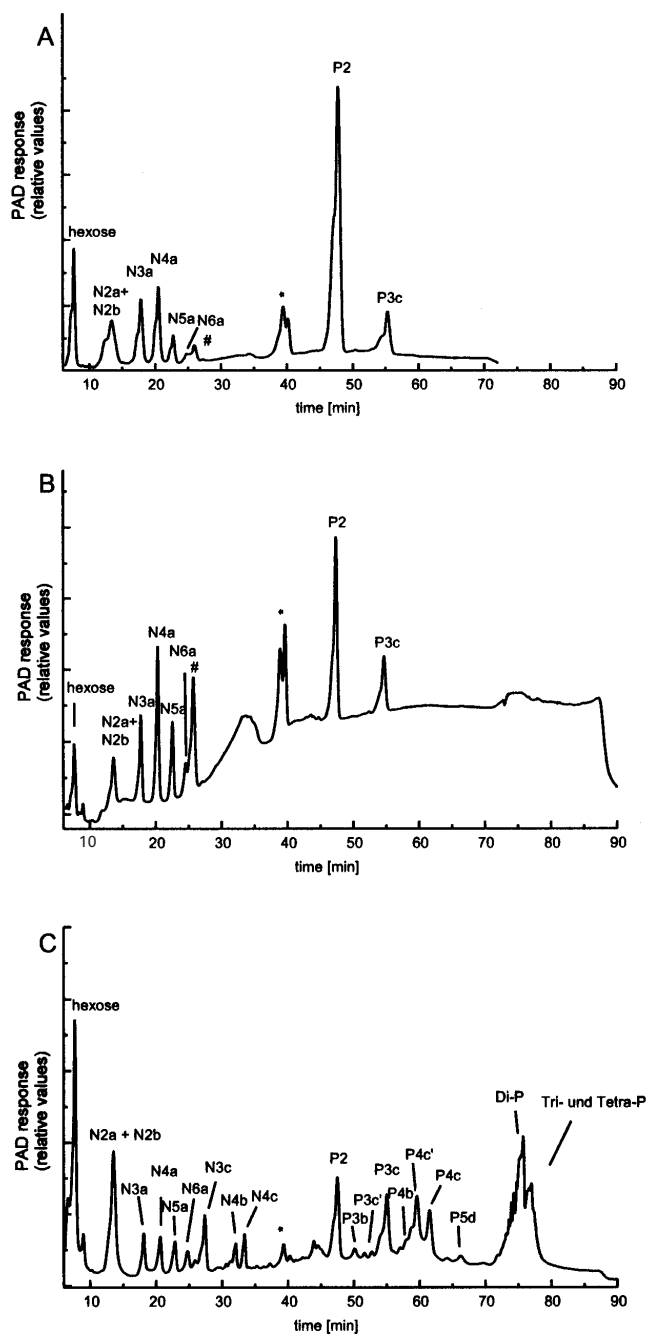
Figure 7   HPAE-HPLC profiles of *L. mexicana* SAP, pPPG2 and aPPG neutral and phosphorylated glycans

Neutral (N) and phosphorylated (P) glycans were released by mild acid hydrolysis from *L. mexicana* SAP (**A**), pPPG2 (**B**) and aPPG (**C**), and resolved on a Carbo Pac PA10 column using gradient program 3. * is a peak containing some partial hydrolysis products and non-carbohydrate contaminants.

Table 3   Glycan structures of *L. mexicana* pPPG2 and SAP

| | | Relative abundance* | | |
| | | Mild acid: pPPG2 | Mild acid: SAP | 40% HF: pPPG2 |
Glycan	Proposed structure			
		Σ: 62.1	Σ: 45.5	n.a.
Hexose		16.4	12.0	7.1
N2a + N2b	Manα1–2Man Galβ1–4Man	9.1	11.0	51.6
N3a	(Manα1–2)$_2$Man	9.2	8.4	8.5
N3c	Glcβ1–3Galβ1–4Man	N.D.	N.D.	13.7
N4a	(Manα1–2)$_3$Man	16.1	9.1	13.0
N5a	(Manα1–2)$_4$Man	8.0	3.0	5.2
N6a	(Manα1–2)$_5$Man	3.3	2.0	1.0
Phosphorylated oligosaccharides (P)		Σ: 37.9	Σ: 54.4	N.A.
P2	PO$_4$-6-Galβ1–4Man	28.3	46.7	N.A.
P3c	PO$_4$-6[Glcβ1–3]Galβ1–4Man	9.6	7.7	N.A.
Ratio N:P		0.6:1	1.2:1	N.A.

* Determined by integration of the PAD signal.
N.D., not detected.
N.A., not applicable.

the aPPG protein backbone [40b] (Table 2) and the compositions obtained earlier from purified aPPG (Table 2).

pPPG2 isolated from *L. mexicana* WT was subjected to mild acid hydrolysis under conditions known to cleave hexose-1-phosphate bonds and to quantitatively release PGs from the PPG protein backbones [18,26,27]. The released oligosaccharides were separated by HPAE-HPLC and the peak pattern was compared to that of mild acid-released SAP glycans: the glycan profiles of pPPG2 preparations were very similar to that of SAP (cf. Figure 7A with Figure 7B), suggesting that these molecules are modified by similar types of glycans. pPPG2 isolated from the *L. mexicana* Δlmsap1/2 mutant showed the same glycan pattern (not shown). The identity of the individual pPPG2 glycans (Table 3) was further confirmed by HPAE-HPLC after Jack bean α-mannosidase and bovine testes β-galactosidase digests of 40% HF-treated pPPG2, which led to complete degradation of N2a, N3a, N4a, N5a, N6a and N2b, respectively (Figures 8C–F). In addition, authentic of N2a, N3a, N4a, N5a, N6a, N2b, P2 and P3c isolated from SAP [25] were added individually to mild acid hydrolysates of pPPG2 prior to HPAE-HPLC analysis to demonstrate coelution in HPAE-HPLC (not shown).

The glycan composition of pPPG2 was, however, markedly different from that of its amastigote-expressed counterpart aPPG. In particular, the multiphosphorylated glycans, some of the monophosphorylated glycans (P3b, P3c′, P4b, P4c′, P4c, P5d) and some of the neutral glycans (N3c, N4b and N4c) were not detected in mild acid hydrolysed pPPG2 (cf. Figure 7B with Figure 7C) and the glycan backbones N4b, N4c, N5c and N5d were absent in 40% HF-treated samples of pPPG2 (cf. Figure 8A with Figure 8B).

pPPG2 contained Ser(P) which was detected by RP-HPLC of PTC-derivatized partial hydrolysates (6 M HCl, 90 min, 110 °C) (data not shown). A more quantitative method to detect Ser(P) residues in peptides and proteins is the conversion to SEC by alkaline β-elimination to dehydroalanine followed by nucleophilic addition of ethanethiol. SEC is then detected and quantified after total protein hydrolysis as a PTC derivative by RP-HPLC [46]. This method was first validated for *L. major* fPPG as a standard compound with known ratio of Ser(P) to Ser [26]. The results of the analysis indicated that about 87.9 mol% of the

appearance. They showed contour lengths of 68.4 ± 7.9 nm and diameters of 24.8 ± 4.6 nm (Figure 4C).

Structural characterization of pPPG2

Amino acid analysis showed that pPPG2 is rich in Ser, Gly, Thr, Ala, Glu/Gln and Pro and that its overall composition is very similar to the composition predicted by the *ppg2* gene encoding
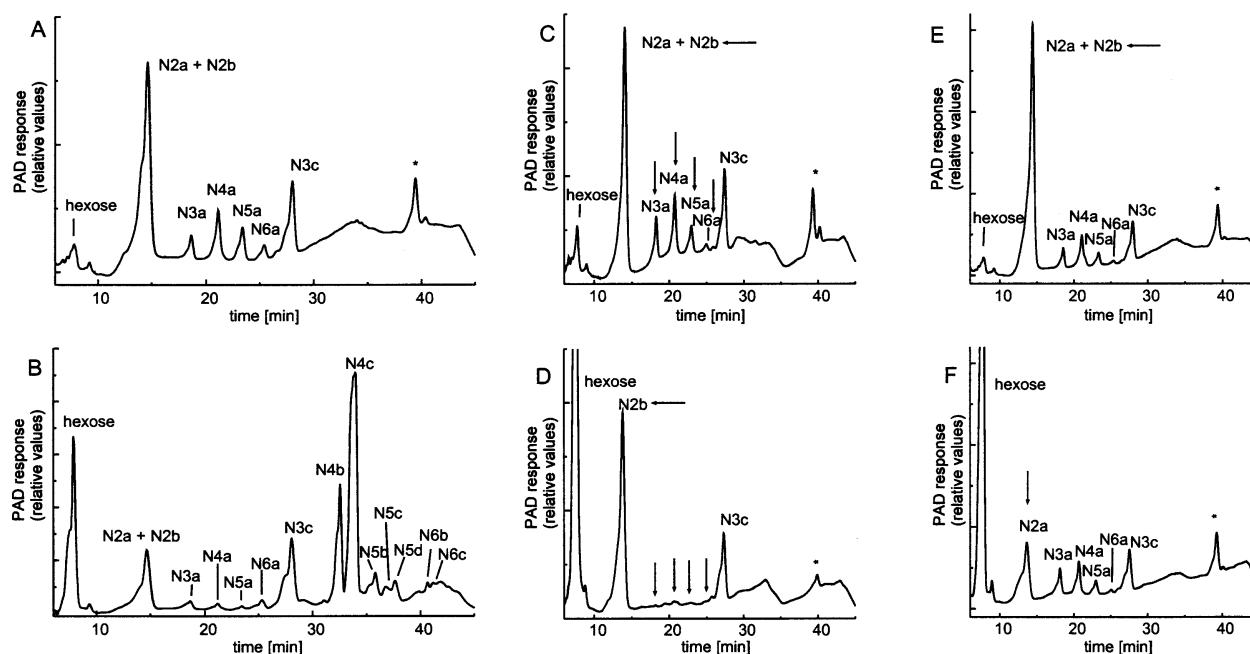
Figure 8 HPAE-HPLC profiles of *L. mexicana* pPPG2 and aPPG glycan backbones released by 40% HF dephosphorylation

Neutral glycans from 40% HF-treated pPPG2 (**A**, **C–F**) and aPPG (**B**) were resolved on a Carbo Pac PA10 column using program 1 before (**A–C**, **E**) and after jack bean α-mannosidase (**D**) or bovine testes β-galactosidase (**F**) treatment. * depicts a non-carbohydrate contaminant.

fPPG Ser residues are phosphorylated (Figure 9A and 9G) which compares well with the previous estimate of 84 mol% based on partial acid hydrolysis of fPPG and detection of released Ser(P) as PTC derivative [26]. The application of this method to pPPG2 and aPPG suggested that 44.6 mol% and 50.5 mol% of their Ser residues were phosphorylated, respectively (Figures 9D, H, I). Almost all Ser(P) (> 98 mol%) in pPPG2, aPPG and fPPG was resistant to alkaline phosphatase (Figures 9B, E, G–I); after mild acid deglycosylation followed by alkaline phosphatase treatment, however, only 25.3, 34.1 and 5.7%, respectively, of the Ser(P) originally present could be detected (Figures 9C, F–I). These results suggests that Ser(P) residues in pPPG2, as in aPPG and fPPG, form alkaline phosphatase-resistant phosphodiesters with PGs as shown in Scheme 2A.

DISCUSSION

It has been shown that virulence of *Leishmania* parasites in the mammalian host requires the biosynthesis of PGs and there is strong evidence that this is also the case for the colonization of the sandfly vector (reviewed in [10,15,16]). *Leishmania* prom-astigotes display the PG-containing molecules LPG [13] and mPPG [35] on their surface. They also release large amounts of PGs present on such molecules as LPG, PG, SAP and fPPG [15,16] into their environment. In this study we have identified pPPG2, a new member of this family of PG-modified molecules which is secreted by *L. mexicana* promastigotes into the culture medium. Purified pPPG2 was obtained by a combination of column chromatography, ultrafiltration and ultracentrifugation and shown to be morphologically and immunologically distinct from SAP and fPPG/mPPG as shown by electron microscopy and application of peptide-specific antibodies. Amino acid analysis of purified pPPG2, however, suggested that it may have the same protein backbone as the secreted amastigote product

aPPG, previously thought to be specific for the mammalian stage parasites [27,34]. This hypothesis was further strengthened by immunological cross-reaction of pPPG2 and aPPG with several antisera directed against the protein backbone of the latter compound and confirmed by cloning and targeted deletion of their common gene *ppg2* [40b]. Major differences between pPPG2 and aPPG, however, were observed with respect to their apparent molecular mass, their ultrastructure and their sensitivity to proteases. Our results suggest that this may be a consequence of stage-specific glycosylation of the common protein backbone: the molar ratio of amino acids to phosphate in pPPG2 is approx. 3:1. Assuming a molar ratio of hexose to phosphate of 2.5:1 it is estimated that pPPG2 contains approx. 39% (w/w) protein, 11% (w/w) phosphate and 50% (w/w) carbohydrate and therefore displays considerably fewer PGs than aPPG, which consists of 14.5% (w/w) protein, 15.5% (w/w) phosphate and 70% (w/v) carbohydrate [34]. Interestingly, the large difference in PG content between aPPG and pPPG2 appears not to be caused by a lower degree of serine phosphoglycosylation in the latter compound (50.5 mol% vs. 44.6 mol%) but by the addition of shorter and less complex structures. In pPPG2, about 50% of the Ser(P)-linked glycans are simple mannooligosaccharide cap structures ([Manα1–2]$_{0-5}$Man while the rest contain on average only one additional monophosphorylated glycan ([±Glcβ1-3]PO$_4$-6-Galβ1–4Man). This may also explain the failure of pPPG2 to react with the mAb LT6. In contrast, aPPG displays highly branched and complex glycan chains consisting, on average, of 6 mono- or multiphosphorylated glycans and 4 cap oligosaccharides [27].

It has been shown that heavily O-glycosylated domains in mammalian mucins (reviewed in [47]) as well as the Ser-O-phosphoglycosylated domain of *L. mexicana* SAP2 [48] form extended filamentous polypeptide chains that exhibit contour lengths of 230–260 pm/amino acid. The sequence of the *ppg2*
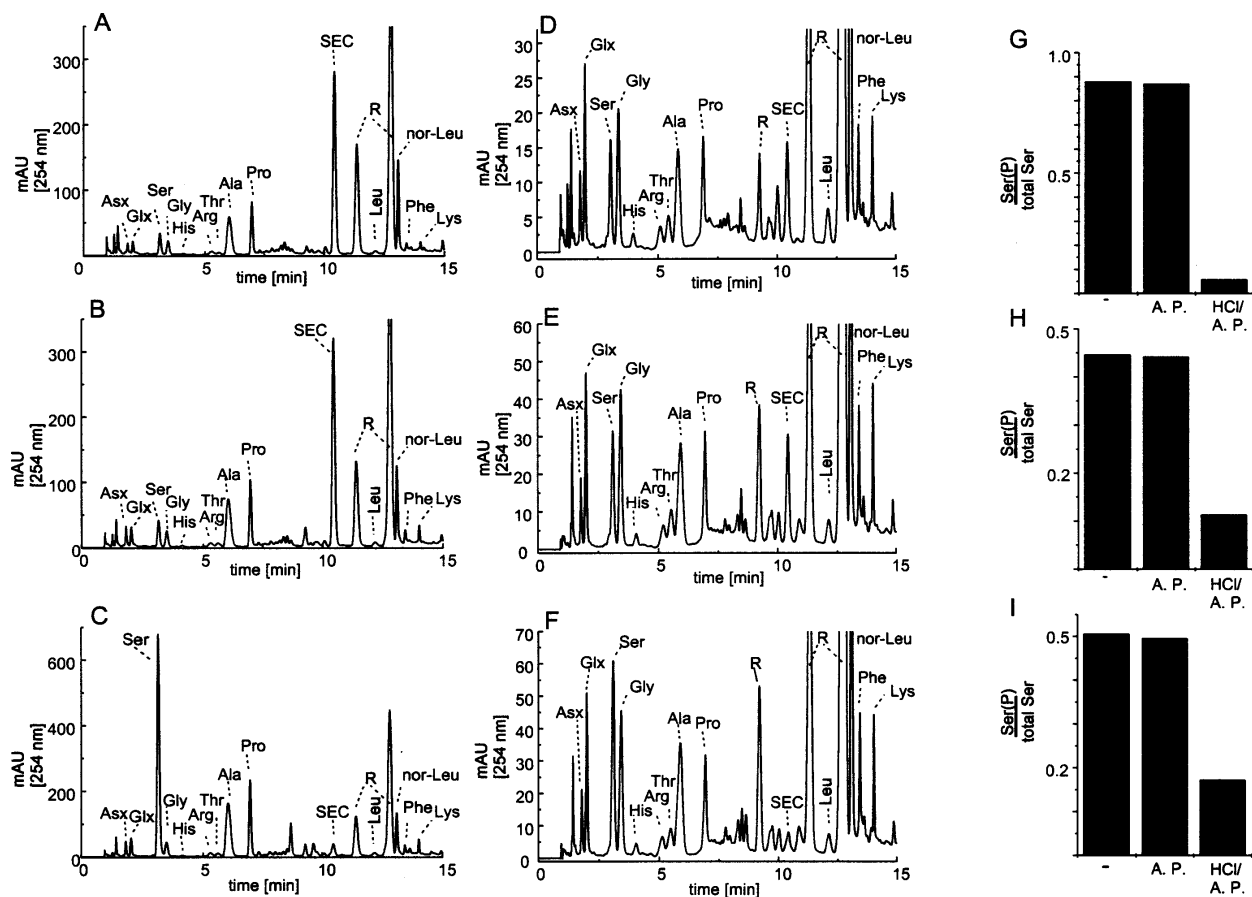
Figure 9   Quantitative determination of phosphoserine-derived *S*-ethylcysteine in total hydrolysates of modified *L. major* fPPG, *L. mexicana* pPPG2 and *L. mexicana* aPPG

L. major fPPG, *L. mexicana* pPPG2 and *L. mexicana* aPPG were subjected to NaOH-catalysed β-elimination of P-Ser. The resulting dehydroalanine was converted to SEC by the addition of ethanethiol. Amino acids from total hydrolysates (6 M HCl, 20 h, 110 °C) were converted to their phenylthiocarbamyl derivatives and resolved on a Pico-tag column. Nor-leucine (nor-Leu) was added as an internal standard. (**A**) *L. major* fPPG, no pretreatment. (**B**) *L. major* fPPG, digestion with alkaline phosphatase (A.P.). (**C**) *L. major* fPPG, mild acid hydrolysis followed by digestion with A.P. (HCl/A.P.) (**D**) *L. mexicana* pPPG2, no pretreatment. (**E**) *L. mexicana* pPPG2, A.P. (**F**) *L. mexicana* pPPG2, HCL/A.P. (**G–I**) Ser(P)/total Ser ratios from fPPG (**G**), pPPG2 (**H**) and aPPG (**I**) calculated from chromatograms **A–F** and from data not shown (**I**).

gene predicts a region of 174–198 amino acids consisting of Ser-rich 24 amino acid repeats, which serve as phosphoglycosylation sites [40b]. Assuming a mucin-like structure, these peptide repeats could form filaments extending over 40–50 nm. The contour length of 42.9 ± 3.7 nm measured for a population of purified pPPG2 molecules compares very well with this estimate. In the case of aPPG, the much longer, more complex, and branched glycan chains extending from the protein backbone appear to lead to major changes in ultrastructure compared to pPPG2: electron micrographs of glycerol-sprayed and rotary-shadowed aPPG molecules show that they are about 20–25 nm longer and 15–20 nm thicker than pPPG2 molecules.

These ultrastructural differences may be the reason for the observed differential susceptibility of these molecules to degradation by proteinase K. Whereas the heavily glycosylated aPPG is completely resistant to this enzyme, pPPG2 appears to possess gaps in the surrounding glycocalyx which allow proteinase K access to the peptide backbone resulting in degradation (Scheme 2). On the other hand, antibodies raised against recombinant peptides spanning the entire *ppg2* open reading frame, though capable of strong interactions with the deglycosylated molecules, were unable to recognize the native form of pPPG2 (and aPPG),

suggesting that access to the peptide backbone of pPPG2 is limited to compounds significantly smaller than IgGs, such as proteinase K.

It appears likely that aPPG in the amastigote [34] and pPPG2 in the promastigote are secreted via the flagellar pocket, which is the primary site of endo- and exocytosis in *L. mexicana* [33]; however, the unequivocal identification of the aPPG and pPPG2 secretion pathway by immunofluorescence and immunelectron microscopy is currently not possible due to a lack of specific antibodies that recognize the native forms of the molecules. The peptide-specific antibodies described in this work could not be used in such studies because they were only able to detect deglycosylated aPPG and pPPG2.

Differential glycosylation of the same protein backbone has frequently been observed for mammalian mucins where tissue-specific glycoforms are well-studied. It appears that the primary sequence of mucins does not predetermine glycosylation patterns which may rather be defined by tissue-specific glycosyltransferase and glycosidase expression (reviewed in [47]). In *Leishmania*, life-stage-dependent modifications of glycan structures have been most extensively studied for the lipid-linked PGs of *L. major* LPG, where specific glycoforms are present in procyclic and

Scheme 2   Schematic structure of pPPG2 and aPPG

It has been shown that PGs can be attached in the central 174–198 amino acid repeat region, shown as rods between the N-terminal (NH$_2$) and the C-terminal (COOH) domain of the protein backbone (see [40b]). Whether PGs are also attached outside the repeat region is not known. Also unknown is the detailed structure of individual glycan chains. The much more complex and branched PG chains of aPPG [27] may be responsible for the resistance of this molecule to proteinase K, possibly by completely covering the protein backbone (B), while in pPPG2, the linear and less complex PGs allow proteinase K some access to the polypeptide chain (A).

metacyclic promastigotes as well as in amastigotes (reviewed in [14]). It has been shown that procyclic LPG serves as a ligand for sandfly midgut receptors, a function lost by metacyclic LPG. The LPG glycoform of metacyclic promastigotes, however, confers complement resistance to the parasites, a prerequisite for effective transmission from the sandfly to the mammalian host. The small amounts of *L. major* amastigote-specific LPG may be a ligand for the attachment of the parasites to macrophages (reviewed in [10,15]. In this study we have demonstrated life stage-specific phosphoglycosylation of a defined *L. mexicana* polypeptide encoded by the *ppg2* gene [40b]. The functional significance for the synthesis of different glycoforms of the *ppg2* gene product by *L. mexicana* promastigotes and amastigotes is not yet clear; however, the higher protease resistance of aPPG compared to pPPG2 could conceivably be of importance in the protease-rich environment of the phagolysosomal compartment of host macrophages. Possible functions of the glycoform pPPG2 for the insect

stage promastigotes remain to be defined, but it has been shown that aPPG may be important for the amastigotes as a potent soluble complement activator [40] and as a vacuolizing agent [39]. The availability of purified pPPG2 will allow us to investigate whether these activities of aPPG are dependent on its unique glycosylation, and the recent generation of *ppg2* knockout mutants [40b] will enable us to address functional aspects in promastigotes and amastigotes in greater depth.

REFERENCES

1   Alexander, J. and Russell, D. G. (1992) Adv. Parasitol. **31**, 175–254
2   Bouvier, J., Schneider, P. and Etges, R. (1995) Methods Enzymol. **248**, 614–633

3   Kahl, L. P. and McMahon-Pratt, D. (1987) J. Immunol. **138**, 1587–1595

4   Murray, P. J., Spithill, T. W. and Handman, E. (1989) J. Immunol. **143**, 4221–4226

5   McConville, M. J., Homans, S. W., Thomas-Oates, J. E., Dell, A. and Bacic, A. (1990) J. Biol. Chem. **265**, 7385–7394

6   McConville, M. J. and Blackwell, J. M. (1991) J. Biol. Chem. **266**, 15170–15179

7   McConville, M. J., Collidge, T. A., Ferguson, M. A. J. and Schneider, P. (1993) J. Biol. Chem. **268**, 15595–15604

8   Schneider, P., Rosat, J. P., Ransijn, A., Ferguson, M. A. J. and McConville, M. J. (1993) Biochem. J. **295**, 555–564

9   Zawadzki, J., Scholz, C., Currie, G., Coombs, G. H. and McConville, M. J. (1998) J. Mol. Biol. **282**, 287–299

10   Mengeling, B. J., Beverley, S. M. and Turco, S. J. (1997) Glycobiology, **7**, 873–880

11   Handman, E., Greenblatt, C. L. and Goding, J. W. (1984) EMBO J. **3**, 2301–2306

12   Greis, K. D., Turco, S. J., Thomas, J. R., McConville, M. J., Homans, S. W. and Ferguson, M. A. J. (1992) J. Biol. Chem. **267**, 5876–5881

13   Turco, S. J. and Descoteaux, A. (1992) Annu. Rev. Microbiol. **46**, 65–94

14   McConville, M. J. and Ferguson, M. A. J. (1993) Biochem. J. **294**, 305–324

15   Ilg, T., Handman, E., Ng, K., Stierhof, Y.-D. and Bacic, A. (1999) Trends Glycosci. Glycotech. **11**, 1–19

16   Ilg, T., Handman, E. and Stierhof, Y.-D. (1999) Biochem. Soc. Trans., **27**, 48–55

17   Kaneshiro, E., Gottlieb, M. and Dwyer, D. M. (1982) Infect. Immun. **37**, 558–567

18   Turco, S. J., Wilkerson, M. A. and Clawson, D. R. (1984) J. Biol. Chem. **259**, 3883–3889

19   Turco, S. J., Orlandi, P. A., Homans, S. W., Ferguson, M. A. J., Dwek, R. A. and Rademacher, T. W. (1989) J. Biol. Chem. **264**, 6711–6715

20   Thomas, J. R., McConville, M. J., Thomas-Oates, J. E., Homans, S. W., Ferguson, M. A. J., Gorin, P. A. J., Greis, K. D. and Turco, S. J. (1992) J. Biol. Chem. **267**, 6829–6833

21   McConville, M. J., Thomas-Oates, J., Ferguson, M. A. J. and Homans, S. W. (1990) J. Biol. Chem. **265**, 19611–19623

22   McConville, M. J., Schnur, L. F., Jaffe, C. and Schneider, P. (1995) Biochem. J. **310**, 807–818

23   Ilg, T., Etges, R., Overath, P., McConville, M. J., Thomas-Oates, J., Thomas, J., Homans, S. W. and Ferguson, M. A. J. (1992) J. Biol. Chem. **267**, 6834–6840

24   Descoteaux, A. and Turco, S. J. (1993) Parasitol. Today **9**, 468–471

25   Ilg, T., Overath, P., Ferguson, M. A. J., Rutherford, T., Campbell, D. G. and McConville, M. J. (1994) J. Biol. Chem. **269**, 24073–24081

26   Ilg, T., Stierhof, Y.-D., Craik, D., Simpson, R., Handman, E. and Bacic, A. (1996) J. Biol. Chem. **271**, 21583–21596

27   Ilg, T., Craik, D., Currie, G., Multhaup, G. and Bacic, A. (1998) J. Biol. Chem. **273**, 13509–13523

28   Mehta, D. P., Ichikawa, M., Salimath, P. V., Etchison, J. R., Haak, R., Manzi, A. and Freeze, H. H. (1996) J. Biol. Chem. **271**, 10897–10903

29   Jaffe, C. L., Perez, L. and Schnur, L. F. (1990) Mol. Biochem. Parasitol. **41**, 233–240

30   Bates, P. A., Hermes, I. and Dwyer, D. M. (1990) Mol. Biochem. Parasitol. **39**, 247–255

31   Ilg, T., Menz, B., Winter, G., Russell, D. G., Etges, R., Schell, D. and Overath, P. (1991) J. Cell Sci. **99**, 175–180

32   Ilg, T., Stierhof, Y. D., Etges, R., Adrian, M., Harbecke, D. and Overath, P. (1991) Proc. Natl. Acad. Sci. U.S.A. **88**, 8774–8778

33   Stierhof, Y.-D., Ilg, T., Russell, D. G., Hohenberg, H. and Overath, P. (1994) J. Cell Biol. **125**, 321–331

34   Ilg, T., Stierhof, Y.-D., McConville, M. J. and Overath, P. (1995) Eur. J. Cell Biol. **66**, 205–215

35   Ilg, T., Montgomery, J., Stierhof, Y.-D. and Handman, E. (1999) J. Biol. Chem., in press

36   Stierhof, Y.-D., Schwarz, H., Menz, B., Russell, D. G., Quinten, M. and Overath, P. (1991) J. Cell Sci. **99**, 181–186

37   Ilg, T. (1992) Ph.D. thesis, Universität Tübingen

38   Stierhof, Y.-D., Bates, P. A., Jacobson, R., Schlein, Y., Rogers, M., Handman, E. and Ilg, T. (1999) Eur. J. Cell Biol. **78**, 675–689

39   Peters, C., Stierhof, Y.-D. and Ilg, T. (1997) Infect. Immun. **65**, 783–786

40a Peters, C., Kawakami, M., Kaul, M., Ilg, T., Overath, P. and Aebischer, T. (1997) Eur. J. Immunol. **27**, 2666–2672

40b Göpfert, U., Goehring, N., Klein, C. and Ilg, T. (1999) Biochem. J. **344**, 787–795.

41   Menz, B., Winter, G., Ilg, T., Lottspeich, F. and Overath, P. (1991) Mol. Biochem. Parasitol. **47**, 101–108

42   Wiese, M., Ilg, T., Lottspeich, F. and Overath, P. (1995) EMBO J. **14**, 1067–1074

43   Laemmli, U. K. (1970) Nature **227**, 680–685

44   Ilg, T., Harbecke, D., Wiese, M. and Overath, P. (1993) Eur. J. Biochem. **217**, 603–615

45   Oxley, D. and Bacic, A. (1995) Glycobiology **5**, 517–523

46   Meyer, H. E., Hoffmann-Posorske, E. and Heilmeyer, L. M. (1991) Methods Enzymol. **201**, 169–185

47   Gendler, S. J. and Spicer, A. P. (1995) Annu. Rev. Physiol. **57**, 607–634

48   Stierhof, Y.-D., Wiese, M., Ilg, T., Overath, P., Haener, M. and Aebi, Ue. (1998) J. Mol. Biol. **282**, 137–148